NUMERICAL RESONANCES FOR SCHOTTKY SURFACES VIA LAGRANGE–CHEBYSHEV APPROXIMATION

OSCAR F. BANDTLOW, ANKE POHL, TORBEN SCHICK, AND ALEXANDER WEISSE

Dedicated to Professor Manfred Denker on the occasion of his 75th birthday

ABSTRACT. We present a numerical method to calculate resonances of Schottky surfaces based on Selberg theory, transfer operator techniques and Lagrange–Chebyshev approximation. This method is an alternative to the method based on periodic orbit expansion used previously in this context.

1. INTRODUCTION AND STATEMENT OF RESULTS

In numerical experiments, Borthwick noticed that for some classes of Schottky surfaces the sets of resonances exhibit rather curious and unexpected patterns [Bor14], an observation that triggered a series of further investigations, e.g., [BW16, PV19]. The numerics used in these articles is based on the method of periodic orbit expansion. With this article we present an alternative method, based on Lagrange–Chebyshev approximation with adapted domains. We briefly survey both methods and our main results in this section, referring to the next sections for details and precise definitions.

Let X be a Schottky surface, i.e., a hyperbolic surface whose fundamental group Γ is a (Fuchsian) Schottky group. The resonances of X are the poles of the extension of the resolvent

$$R(s) := \left(\Delta_X - s(1-s) \right)^{-1} \colon C_c^\infty(X) \to C^\infty(X), \quad \operatorname{Re} s \gg 1 \,,$$

of the Laplacian Δ_X of X to a meromorphic family $s \mapsto R(s)$ on all of $\mathbb{C}$. As is well-known by now, the Hausdorff dimension δ of the limit set $\Lambda(X)$ of X constitutes a threshold in $\mathbb{C}$ with respect to the location of the resonances of X: the half-space $\{s \in \mathbb{C} \mid \operatorname{Re} s > \delta\}$ does not contain any resonances, the point δ itself is a resonance (with multiplicity 1), the *critical axis* $\{s \in \mathbb{C} \mid \operatorname{Re} s = \delta\}$ contains no further resonance, the half-space $\{s \in \mathbb{C} \mid \operatorname{Re} s < \delta\}$ contains infinitely many resonances, and $\{\operatorname{Re} s \mid s \text{ a resonance}\}$ is unbounded from below. Several further results on the location and distribution of the resonances for Schottky surfaces have been established, some of them very recently, see, e.g., [GZ95, GZ97, BD18, PS18, NM19].

The study of resonances of Schottky surfaces is not just interesting from a theoretical point of view, their properties are also of considerable interest in applications, e.g., [BGS11, OW16]. In spite of intensive efforts, however, many questions

concerning the nature of the resonances are still wide open to date, including several very elementary ones. Numerical investigations of the resonance sets might lead to new insights, and are therefore clearly called for. In addition, as we will see in this paper, their investigation is also rewarding from a numerical point of view.

Both numerical methods that we will discuss crucially rely on the interpretation of resonances using dynamical zeta functions and transfer operators. The dynamical zeta function of interest to us is the Selberg zeta function Z_X of X, which is an entire function given by the infinite product

$$Z_X(s) = \prod_{\ell \in L(X)} \prod_{k=0}^{\infty} \left(1 - e^{-(s+k)\ell}\right)$$

for $s \in \mathbb{C}$ with $\operatorname{Re} s \gg 1$, and by analytic continuation of this infinite product on all of $\mathbb{C}$. Here, $L(X)$ denotes the primitive geodesic length spectrum of X including multiplicities. The resonances of X constitute the main bulk of the zeros of Z_X (including multiplicities); the additional zeros of Z_X are the well-understood and comparatively sparse so-called topological zeros [PP01]. Thus, searching for the resonances of X is essentially equivalent to searching for the zeros of Z_X.

The Selberg zeta function can be represented as the Fredholm determinant of a transfer operator family $(\mathcal{L}_s)_{s \in \mathbb{C}}$, acting on a suitable function space $\mathcal{H}$. Thus, for all $s \in \mathbb{C}$,

$$(1) \qquad Z_X(s) = \det(1 - \mathcal{L}_s) \,.$$

(We refer to Section 2.4 for the definition of the transfer operators $\mathcal{L}_s$.) In turn, searching for the zeros of Z_X, and hence essentially for the resonances of X, translates to searching for the values of the parameter s of the transfer operator $\mathcal{L}_s$ such that $\det(1 - \mathcal{L}_s) = 0$.

The *method of periodic orbit expansion*, employed by Borthwick for the numerical approximation of resonances, takes advantage of the identity in (1) to deduce the series expansion

$$(2) \qquad Z_X(s) = 1 + \sum_{n=1}^{\infty} d_n(s) \,,$$

where $d_0(s) = 1$ and

$$(3) \qquad d_n(s) = -\frac{1}{n} \sum_{k=1}^{n} d_{n-k}(s) \operatorname{Tr} \mathcal{L}_s^k$$

for $n \in \mathbb{N}$. The traces $\operatorname{Tr} \mathcal{L}_s^k$ are of the form

$$(4) \qquad \operatorname{Tr} \mathcal{L}_s^k = \sum_{\ell \in L_k(X)} \frac{e^{-s\ell}}{1 - e^{-\ell}} \,,$$

where $L_k(X)$ is a finite multiset of lengths of periodic geodesics on X, with lengths growing with k, and $\#L_k(X) \sim c^k$ for some $c > 0$. Truncating the series in (2) at $N \in \mathbb{N}$ leads to

$$Z_N(s) = 1 + \sum_{n=1}^{N} d_n(s) \,,$$

the zeros of which approximate the zeros of Z_X.

Borthwick's primary goal was to study the resonances of X near the critical axis $\{s \in \mathbb{C} \mid \operatorname{Re} s = \delta\}$, for which the periodic orbit expansion method is well-suited. In addition to the rather surprising results he obtained, he also reported limitations of this method for the investigation of resonances further away from the critical axis (e.g., resonances s with $\operatorname{Re} s < 0$) as well as for Schottky surfaces with Euler characteristic $\chi(X) < -1$ (equivalent to Γ having more than 2 generators) or with small funnel widths (i.e., for δ near 1), see [Bor14]. The main cause of the limitations is the high computational cost of the recursions in (3) as well as that of the sums in (4), the number of summands of which grow exponentially with k and polynomially with $-\chi(X)$, and which need to be almost completely redone for every single s.

For *highly symmetric* Schottky surfaces, the Venkov–Zograf factorization formulas for Selberg zeta functions can be applied to reduce the computational cost of the periodic orbit expansion method making it possible to consider, for example, some Schottky surfaces with 4 funnels, that is, with Euler characteristic -2, see [BW16]. Qualitatively, however, the limitations remain.

The method we present here is inspired by Nyström's approach [Nys30] to solve Fredholm-type integral equations. The definition of the transfer operator $\mathcal{L}_s$ introduced above leaves room for possible choices of the function space $\mathcal{H}$. While the periodic orbit expansion method is not affected by the choice of a suitable $\mathcal{H}$, our method heavily depends on it; in fact, it takes advantage of this option, reconsidering the choice during investigations and adapting it to specific situations.

The starting point of this method is a careful first choice of the function space $\mathcal{H}$ on which we consider the transfer operator $\mathcal{L}_s$ and approximate the functions $f \in \mathcal{H}$ using Lagrange–Chebyshev interpolation. On approximated functions, $\mathcal{L}_s$ then acts as a *finite* matrix M_s, and $\det(1 - M_s)$ serves as an approximation of the Selberg zeta function $Z_X(s)$ at $s \in \mathbb{C}$. The evaluation of $\det(1 - M_s)$ in turn is facilitated by the existence of highly optimized algorithms for the calculation of determinants. Moreover, the specific structure of M_s (see Section 4) makes it possible to reuse a substantial part of previously computed values when changing s.

To further improve the approach we take advantage of the possibility to change $\mathcal{H}$ and pick a sequence of function spaces $(\mathcal{H}_m)_{m \in \mathbb{N}}$ such that along any sequence $(f_m)_{m \in \mathbb{N}}$ with $f_m \in \mathcal{H}_m$, $m \in \mathbb{N}$, the domains of the functions shrink and converge to the limit set $\Lambda(X)$ of X. By using a space of this sequence with sufficiently refined domains, we can take advantage of the geometry and dynamics of X to investigate the resonances of X over a wider range of parameters.

This method, termed *domain-refined Lagrange–Chebyshev approximation*, pushes further the frontier of numerical investigations of resonances for Schottky surfaces.

Observation. *With the method of domain-refined Lagrange–Chebyshev approximation, resonances can be calculated efficiently also further into the negative half-space $\{s \in \mathbb{C} \mid \operatorname{Re} s < 0\}$ as well as for Schottky surfaces with several generators and with small funnel widths. This method is not restricted to Schottky surfaces with additional symmetries or any other specific properties.*

The basic idea of discretizing operators by expansions in orthogonal polynomials and approximating Fredholm determinants by matrix determinants already has a rather long history and in principle dates back to Ritz, Galerkin [GW12] and Nyström [Nys30]. The review of Bornemann [Bor10] gives a nice overview on the

topic and discusses examples from random matrix theory, among others. The approach was also applied successfully to integrable quantum systems [DGK14], where correlation functions are calculated with the help of quantum transfer matrices. In the realm of transfer operators it was used, e.g., in [Fra12, Fra17], mostly applying a monomial basis, leading to new theoretical results [BFM13]. Also computation schemes for transfer operators focusing on Chebyshev polynomials exist already, albeit without discussing their Fredholm determinants, e.g., [Nie16, Wor19, BS20]. The main new aspect of our approach is the domain-refinement, which leads to a particularly efficient basis for the discretized transfer operator. In this article, we focus on presenting the numerical method. We will discuss its validity, error estimates and convergence rates in a forthcoming article.

2. Schottky surfaces, resonances, classical transfer operators

2.1. **Schottky surfaces.** Schottky surfaces are those hyperbolic surfaces for which the fundamental group is a (Fuchsian) Schottky group. Equivalently, these are the geometrically finite, conformally compact, infinite-area hyperbolic surfaces without orbifold singularities or, also equivalently, the hyperbolic surfaces for which the fundamental group is geometrically finite, convex cocompact, non-cocompact and torsion-free. Every Schottky surface can be obtained by a certain geometric construction algorithm [But98], which we will briefly recall in what follows. This algorithm constructs a fundamental domain for every Schottky surface; the side-pairing elements of the fundamental domain and their relations provide a presentation of the fundamental group of the Schottky surface. All hyperbolic surfaces arising from this construction are indeed Schottky.

2.1.1. *Preliminaries for the construction.* As model for the hyperbolic plane we use throughout the upper half-plane

$$\mathbb{H} := \{z \in \mathbb{C} \ : \ \mathrm{Im}\, z > 0\}, \qquad ds_z^2 := \frac{dz\, d\bar{z}}{(\mathrm{Im}\, z)^2}\,,$$

and we identify its group $\mathrm{Isom}^+(\mathbb{H})$ of orientation-preserving Riemannian isometries with the Lie group $\mathrm{PSL}_2(\mathbb{R}) = \mathrm{SL}_2(\mathbb{R})/\{\pm\mathbb{1}\}$. Here, we denote with $\mathbb{1}$ the matrix $\left(\begin{smallmatrix} 1 & 0 \\ 0 & 1 \end{smallmatrix}\right) \in \mathrm{SL}_2(\mathbb{R})$, and we denote an element in $\mathrm{PSL}_2(\mathbb{R})$ by

$$\begin{bmatrix} a & b \\ c & d \end{bmatrix}$$

if it is represented by the matrix $\left(\begin{smallmatrix} a & b \\ c & d \end{smallmatrix}\right) \in \mathrm{SL}_2(\mathbb{R})$. With all identifications in place, the action of $\mathrm{PSL}_2(\mathbb{R})$ on $\mathbb{H}$ is given by fractional linear transformations, thus

$$g.z = \frac{az+b}{cz+d}$$

for $g = \left[\begin{smallmatrix} a & b \\ c & d \end{smallmatrix}\right] \in \mathrm{PSL}_2(\mathbb{R})$, $z \in \mathbb{H}$.

The hyperbolic plane $\mathbb{H}$ embeds canonically into the Riemann sphere $\widehat{\mathbb{C}} = \mathbb{C} \cup \{\infty\}$. In this embedding, the topological boundary $\partial\mathbb{H} = \mathbb{R} \cup \{\infty\}$ of $\mathbb{H}$ coincides with its geodesic boundary. The action of $\mathrm{PSL}_2(\mathbb{R})$ on $\mathbb{H}$ extends holomorphically
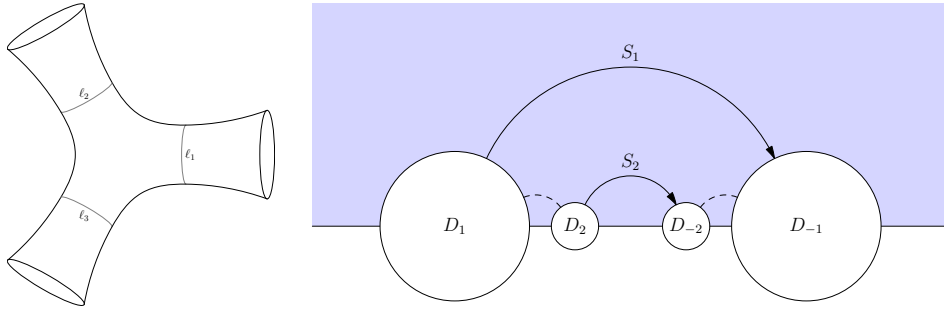
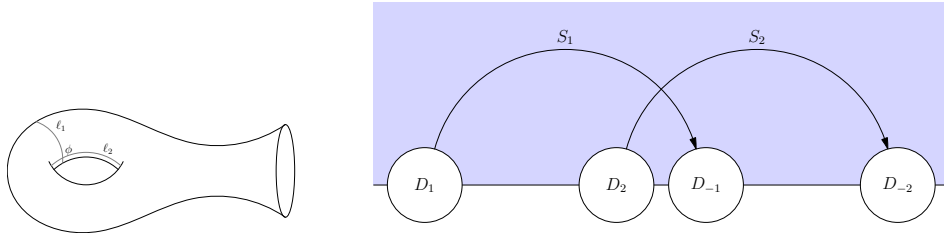FIGURE 1. Construction of a three-funnel surface.

FIGURE 2. Construction of a funneled torus surface.

to all of $\widehat{\mathbb{C}}$. The extended action is given by

$$
g.z = \begin{cases} \infty & \text{if } z = \infty, c = 0, \text{ and if } z \neq \infty, cz + d = 0, \\ \frac{a}{c} & \text{if } z = \infty, c \neq 0, \\ \frac{az+b}{cz+d} & \text{otherwise} \end{cases}
$$

for $g = \begin{bmatrix} a & b \\ c & d \end{bmatrix} \in \mathrm{PSL}_2(\mathbb{R})$ and $z \in \widehat{\mathbb{C}}$.

2.1.2. *Geometric construction of Schottky surfaces.* In order to construct a Schottky surface X of Euler characteristic $\chi(X) = 1 - q$ (note that $q \in \mathbb{N}$), we choose $2q$ open Euclidean disks in $\mathbb{C}$ with centers in $\mathbb{R}$ and pairwise disjoint closures. We further fix a pairing of these disks, indicated by indices in $I_G := \{\pm 1, \ldots, \pm q\}$ with opposite signs, say

$$
D_1, D_{-1}, \ldots, D_q, D_{-q}.
$$

We emphasize that the numeration of these disks implied by their indices is not related to their relative positions in $\mathbb{C}$. For each $j \in \{1, \ldots, q\}$ we choose an element S_j in $\mathrm{PSL}_2(\mathbb{R})$ that maps the exterior of the disk D_j to the interior of the disk D_{-j}. For examples see Figures 1 and 2. The subgroup

$$
\Gamma = \langle S_1, \ldots, S_q \rangle
$$

of $\mathrm{PSL}_2(\mathbb{R})$ generated by $S_1, \ldots, S_q$ is a *Schottky group*, and the orbit space $X = \Gamma \backslash \mathbb{H}$ is a *Schottky surface* with Euler characteristic $1 - q$. The subset

$$
\mathcal{F} := \bigcap_{k \in I_G} \left(\mathbb{H} \smallsetminus D_k \right)
$$

of $\mathbb{H}$ is a closed fundamental domain for X with side-pairings given by the elements $S_1, \ldots, S_q$. Note that the set of relations among $S_1, \ldots, S_q$ is empty.

For further use we set

$$S_{-j} := S_j^{-1}$$

for $j \in \{1, \ldots, q\}$, and we call the tuple

$$\left(q, (D_k)_{k \in I_G}, (S_k)_{k \in I_G} \right)$$

Schottky data for X. We remark that different Schottky data may give rise to the same Schottky surface, and indeed any given Schottky surface admits uncountably many choices of Schottky data. We also remark that the notion of Schottky data in [APW18] is slightly more general; the additional freedom allowed there for the choices of the disk family will not be needed for our purposes.

2.2. **Resonances.** The *resonances* of a Schottky surface X are the poles of the meromorphic continuation of the resolvent of its Laplacian. To be more precise, we recall that the Laplace operator

$$\Delta_{\mathbb{H}} := -y^2 \left(\partial_x^2 + \partial_y^2 \right)$$

on $\mathbb{H}$ (here, $z = x + iy \in \mathbb{H}$, $x, y \in \mathbb{R}$) induces the Laplace operator

$$\Delta_X \colon L^2(X) \to L^2(X)$$

on X. The resolvent

(5) $$R_X(s) := \left(\Delta_X - s(1-s) \right)^{-1} \colon L^2(X) \to L^2(X)$$

of Δ_X is defined for all $s \in \mathbb{C}$ with $\operatorname{Re} s > \frac{1}{2}$ for which $s(1-s)$ is not an L^2-eigenvalue of Δ_X. As shown in [MM87, GZ95], the restriction of the family of maps in (5) to $C_c^\infty(X) \to C^\infty(X)$ extends to a meromorphic family

$$R_X(s) \colon L_{\mathrm{comp}}^2(X) \to H_{\mathrm{loc}}^2(X)$$

on all of $\mathbb{C}$. The poles of R_X are the resonances of X. We let $R(X)$ denote the multiset of resonances of X (thus, resonances are included with multiplicities, i.e., the rank of the residue of R_X at the resonance).

2.3. **Selberg zeta function.** For any Schottky surface X we denote by $L(X)$ its multiset of lengths of primitive periodic geodesics (thus, the prime geodesic length spectrum including multiplicities). Further we denote by $\Lambda(X)$ the limit set of X. We recall that $\Lambda(X)$ is the set of limit points (i.e., accumulation points) in the Riemann sphere $\widehat{\mathbb{C}}$ of the orbit $\Gamma.z$ for some (and hence any) $z \in \mathbb{H}$ and any realization Γ of the fundamental group of X in $\mathrm{PSL}_2(\mathbb{R})$. As is well-known, $\Lambda(X)$ is a subset of $\partial \mathbb{H} = \mathbb{R} \cup \{\infty\}$. We let $\delta = \delta(X)$ denote the Hausdorff dimension of $\Lambda(X)$, which for Schottky surfaces can be any value in $[0, 1)$.

The *Selberg zeta function* Z_X of X is given by the infinite product

(6) $$Z_X(s) = \prod_{\ell \in L(X)} \prod_{k=0}^\infty \left(1 - e^{-(s+k)\ell} \right)$$

for $s \in \mathbb{C}$ with $\operatorname{Re} s > \delta$ (where this infinite product converges compactly), and beyond this range by the holomorphic continuation of (6) to all of $\mathbb{C}$. The multiset of zeros of Z_X consists of the multiset $R(X)$ of resonances of X and the *topological*

zeros. The latter are well-understood: they are located at $-\mathbb{N}_0$ with well-known multiplicities. For proofs and more details we refer to the original articles [PP01] as well as [BJP05]. (We remark that the relation between resonances and topological zeros of Selberg zeta functions is reminiscent of the relation between trivial and nontrivial zeros of the Riemann zeta function.)

2.4. **Transfer operators.** The choice of Schottky data

$$\mathcal{S} := \left(q, \left(D_k \right)_{k \in I_G}, \left(S_k \right)_{k \in I_G} \right)$$

for a Schottky surface X allows us to construct a Ruelle-type transfer operator family whose underlying discretization of the geodesic flow on X arises from a Koebe–Morse coding based on the fundamental domain induced by $\mathcal{S}$. We refer to [Bor16] for details and proofs, and present here only the resulting transfer operators and their properties.

To simplify notation, for $s \in \mathbb{C}$, any subset $U \subseteq \mathbb{R}$, any function $f \colon U \to \mathbb{C}$ and any element $g = \left[\begin{smallmatrix} a & b \\ c & d \end{smallmatrix} \right] \in \mathrm{PSL}_2(\mathbb{R})$ we set

$$\tau_s(g^{-1})f(x) := \left(g'(x) \right)^s f(g.x) = |cx + d|^{2s} f\left(\frac{ax+b}{cx+d} \right) \qquad (x \in U)$$

whenever this is well-defined. We will also use holomorphic extensions of this definition to functions defined on open subsets of $\mathbb{C}$ (e.g., the disks D_k, $k \in I_G$). We omit the discussion of the possible choices of holomorphic extensions, in particular of the choices for the logarithm, which heavily depend on the Schottky data and on the required combinations of functions f and group elements g in the Schottky group. None of the stated results depend on these choices. We continue to denote the holomorphic extensions by τ_s or, more precisely, by $\tau_s(g^{-1})f$.

The *transfer operator* $\mathcal{L}_s$ with parameter $s \in \mathbb{C}$ associated to $\mathcal{S}$ is defined formally by

$$(7) \qquad \mathcal{L}_s := \sum_{k \in I_G} 1_{D_k} \cdot \sum_{\substack{j \in I_G \\ j \neq -k}} \tau_s(S_j),$$

where 1_{D_k} denotes the characteristic function of D_k.

The choice of function space on which to consider the transfer operator $\mathcal{L}_s$ is guided by the required applications and may be a subtle task. For Selberg zeta functions there are several good choices of which we present a few in what follows. In Section 3 below we will present some more spaces crucial for our investigations. Throughout, we will denote all transfer operators by $\mathcal{L}_s$, independently of the function space on which they are considered to act.

One common choice, widely used in the study of resonances of Schottky surfaces via transfer operators [GLZ04, Bor16], is the *Hilbert–Bergman space* given by

$$(8) \qquad \mathcal{H} := \bigoplus_{k \in I_G} \mathcal{H}(D_k),$$

where

$$\mathcal{H}(D_k) := \left\{ f \colon D_k \to \mathbb{C} \text{ holomorphic } : \int_{D_k} |f(z)|^2 \, d\lambda(z) < \infty \right\}$$

is the Hilbert space of holomorphic square-integrable functions on D_k, endowed with the standard L^2-inner product. Here, $d\lambda$ denotes the Lebesgue measure on $\mathbb{C}$.

Another common choice, already used by Ruelle [Rue78] and Mayer [May90, May91] in their seminal investigations of Selberg zeta functions via transfer operators, is the *disk algebra* $\mathcal{B}$ associated to $\mathcal{S}$. This is the Banach space

$$\mathcal{B} = \bigoplus_{k \in I_G} A_\infty(D_k), \tag{9}$$

where

$$A_\infty(D_k) := \left\{ f \colon D_k \to \mathbb{C} \text{ holomorphic } : \ f \text{ extends continuously to } \overline{D}_k \right\}$$

is the Banach space of holomorphic functions on D_k that are restrictions of continuous functions on the closure $\overline{D}_k$ of D_k, endowed with the supremum norm.

On the spaces in (8) or in (9) (as well as many other spaces), the transfer operator $\mathcal{L}_s$ is a well-defined self-map, a nuclear operator of order 0 (thus, trace class on $\mathcal{H}$) and its Fredholm determinant equals the Selberg zeta function of X, thus

$$Z_X(s) = \det(1 - \mathcal{L}_s)$$

for all $s \in \mathbb{C}$ (see, e.g., [Bor16] and [FP20]). Therefore, with either of these spaces as domain, the transfer operator $\mathcal{L}_s$ has an eigenfunction with eigenvalue 1 if and only if s is a zero of Z_X. See, e.g., [GGK00].

3. Domain-refined transfer operators

Throughout let X be a Schottky surface,

$$\mathcal{S} = \left(q, \left(D_k \right)_{k \in I_G}, \left(S_k \right)_{k \in I_G} \right)$$

a choice of Schottky data for X, and $(\mathcal{L}_s)_{s \in \mathbb{C}}$ the associated transfer operator family. In Section 2.4 we have exhibited two classes of function spaces that are by now "classical" domains for the transfer operator $\mathcal{L}_s$. Both spaces consist of functions on the disks D_k, $k \in I_G$. In this section we will construct spaces of functions with smaller domains, a step that will be crucial for our numerical method.

The construction of smaller domains is guided by the following intuition: in order to calculate resonances of X we want to use the Selberg zeta function Z_X and its representation $\det(1 - \mathcal{L}_s)$ as a Fredholm determinant by a transfer operator family on a suitable function space, say H. As can be seen from the infinite product in (6), the function Z_X is determined by the *periodic* geodesics on X. Given any such periodic geodesic $\widehat{\gamma}$ on X and any geodesic γ on $\mathbb{H}$ that represents $\widehat{\gamma}$, the two (time-)endpoints $\gamma(+\infty)$ and $\gamma(-\infty)$ of γ are in the limit set $\Lambda(X)$ of X. Intuitively, the function space H should consist of functions whose domains enclose $\Lambda(X)$ and stay "near" $\Lambda(X)$, the nearer to $\Lambda(X)$ the better the numerics. For the choice of H we need to guarantee that the transfer operators $\mathcal{L}_s$, $s \in \mathbb{C}$, define endomorphisms of H and that the relation $Z_X = \det(1 - \mathcal{L}_s)$ holds. To that end we will start with the disks D_k, $k \in I_G$, as domains for the functions and then use the iterated action of the elements S_k, $k \in I_G$, to obtain a sequence of refined domains converging to $\Lambda(X)$.

We first restrict the discussion of the domains to $\mathbb{R}$ and present the shrinking algorithm on the level of real intervals. We then enlarge the shrunken intervals to domains in $\mathbb{C}$. The construction thus allows for an additional degree of freedom which we will exploit for the construction of suitable function spaces. Figure 3 gives an illustration of the iterated refinement procedure that we describe in what follows.
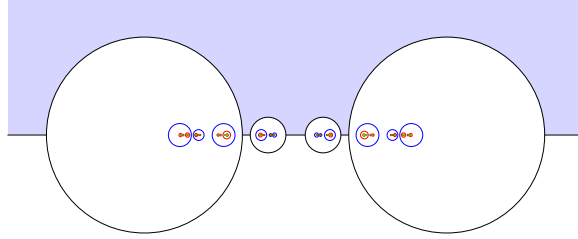

FIGURE 3. Recursive subdivision (for simplicity drawn with disks).

For $k \in I_G$ we let
$$I_k := D_k \cap \mathbb{R}$$
denote the interval in $\mathbb{R}$ that is enclosed by the disk D_k, and we restrict the transfer operator in (7) to these intervals. Thus, again initially only formally,
$$(10) \qquad \mathcal{L}_s = \sum_{k \in I_G} 1_{I_k} \cdot \sum_{j \in I_G \smallsetminus \{-k\}} \tau_s(S_j).$$

For each $n \in \mathbb{N}_0$ we let $\mathcal{W}_n$ denote the set of tuples $(w_1, \ldots, w_n, \ell) \in I_G^{n+1}$ such that $w_k \neq -w_{k-1}$ for all $k \in \{2, \ldots, n\}$ and $\ell \neq w_n$. For each $w = (w_1, \ldots, w_n, \ell) \in \mathcal{W}_n$ we set
$$I_w := S_{w_1} S_{w_2} \cdots S_{w_n}.I_\ell$$
and we let
$$\mathrm{Fct}(I_w; \mathbb{C}) := \{f_w \colon I_w \to \mathbb{C}\}$$
denote the space of complex-valued functions on the interval I_w. Further we let
$$\mathcal{I}_n := \{I_w \ : \ w \in \mathcal{W}_n\}$$
denote the set of *intervals of refinement level* n and we set
$$(11) \qquad \mathrm{Fct}(\mathcal{I}_n; \mathbb{C}) := \bigoplus_{w \in \mathcal{W}_n} \mathrm{Fct}(I_w; \mathbb{C}).$$

The following proposition shows that we may consider the transfer operator $\mathcal{L}_s$ as an operator on $\mathrm{Fct}(\mathcal{I}_n; \mathbb{C})$. We omit the straightforward proof.

Proposition 3.1. *For each $n \in \mathbb{N}$ and $s \in \mathbb{C}$ the transfer operator $\mathcal{L}_s$ in (10) defines a self-map on $\mathrm{Fct}(\mathcal{I}_n; \mathbb{C})$.*

Let $n \in \mathbb{N}$, $s \in \mathbb{C}$ and consider the transfer operator $\mathcal{L}_s$ as an operator on $\mathrm{Fct}(\mathcal{I}_n; \mathbb{C})$. The definition of $\mathrm{Fct}(\mathcal{I}_n; \mathbb{C})$ in (11) as a direct sum of the function spaces $\mathrm{Fct}(I_w; \mathbb{C})$, $w \in \mathcal{W}_n$, yields an identification of $\mathcal{L}_s$ with a matrix
$$(12) \qquad (\mathcal{L}_{s,v,w})_{v,w \in \mathcal{W}_n}$$

where the *matrix coefficient* $\mathcal{L}_{s,v,w}$ for $v, w \in \mathcal{W}_n$ is the unique operator

$$\mathcal{L}_{s,v,w} \colon \operatorname{Fct}(I_w; \mathbb{C}) \to \operatorname{Fct}(I_v; \mathbb{C})$$

such that for all $f, \tilde{f} \in \operatorname{Fct}(\mathcal{I}_n; \mathbb{C}) = \bigoplus \operatorname{Fct}(I_w; \mathbb{C})$ with

$$f = \bigoplus_{w \in \mathcal{W}_n} f_w, \qquad \tilde{f} = \bigoplus_{w \in \mathcal{W}_n} \tilde{f}_w$$

and $\mathcal{L}_s f = \tilde{f}$ we have

$$\tilde{f}_v = \sum_{w \in \mathcal{W}_n} \mathcal{L}_{s,v,w} \, f_w \, .$$

A straightforward calculation allows us to deduce the following explicit formulas for the matrix coefficients.

Proposition 3.2. *Let $s \in \mathbb{C}$.*

    (i) *For $n = 0$ and $v, w \in \mathcal{W}_0 = I_G$ the matrix coefficient $\mathcal{L}_{s,v,w}$ is*

$$\mathcal{L}_{s,v,w} = \begin{cases} \tau_s(S_w) & \text{if } w \neq -v \\ 0 & \text{otherwise.} \end{cases}$$

    (ii) *For $n \geq 1$ and $v = (v_1, \ldots, v_n, \ell_v), w = (w_1, \ldots, w_n, \ell_w) \in \mathcal{W}_n$ the matrix coefficient $\mathcal{L}_{s,v,w}$ is*

$$\mathcal{L}_{s,v,w} = \begin{cases} \tau_s(S_{-w_1}) & \text{if } w = (w_1, v_1, \ldots, v_{n-1}, -v_n) \\ 0 & \text{otherwise.} \end{cases}$$

    With increasing refinement level n, the matrix in (12) representing the transfer operator $\mathcal{L}_s \colon \operatorname{Fct}(\mathcal{I}_n; \mathbb{C}) \to \operatorname{Fct}(\mathcal{I}_n; \mathbb{C})$ becomes sparse with exponentially increasing sparsity.

Example 3.3. We consider a Schottky surface with two generators, say S_1 and S_2. For refinement level 0 the transfer operator $\mathcal{L}_s$ is identified with the matrix

$$(13) \qquad \begin{pmatrix} \tau_s(S_{-2}) & \tau_s(S_{-1}) & \tau_s(S_1) & 0 \\ \tau_s(S_{-2}) & \tau_s(S_{-1}) & 0 & \tau_s(S_2) \\ \tau_s(S_{-2}) & 0 & \tau_s(S_1) & \tau_s(S_2) \\ 0 & \tau_s(S_{-1}) & \tau_s(S_1) & \tau_s(S_2) \end{pmatrix},$$

acting on function vectors of the form

$$\begin{pmatrix} f_{-2} \colon I_{-2} \to \mathbb{C} \\ f_{-1} \colon I_{-1} \to \mathbb{C} \\ f_1 \colon I_1 \to \mathbb{C} \\ f_2 \colon I_2 \to \mathbb{C} \end{pmatrix}.$$

For refinement level 1, the transfer operator $\mathcal{L}_s$ is identified with the matrix

$$(14) \quad \begin{pmatrix}
0 & S_{-2} & 0 & S_{-1} & 0 & 0 & S_1 & 0 & 0 & 0 & 0 & 0 \\
0 & S_{-2} & 0 & S_{-1} & 0 & 0 & S_1 & 0 & 0 & 0 & 0 & 0 \\
0 & S_{-2} & 0 & S_{-1} & 0 & 0 & S_1 & 0 & 0 & 0 & 0 & 0 \\
0 & 0 & S_{-2} & 0 & S_{-1} & 0 & 0 & 0 & 0 & 0 & 0 & S_2 \\
0 & 0 & S_{-2} & 0 & S_{-1} & 0 & 0 & 0 & 0 & 0 & 0 & S_2 \\
0 & 0 & S_{-2} & 0 & S_{-1} & 0 & 0 & 0 & 0 & 0 & 0 & S_2 \\
S_{-2} & 0 & 0 & 0 & 0 & 0 & 0 & S_1 & 0 & S_2 & 0 & 0 \\
S_{-2} & 0 & 0 & 0 & 0 & 0 & 0 & S_1 & 0 & S_2 & 0 & 0 \\
S_{-2} & 0 & 0 & 0 & 0 & 0 & 0 & S_1 & 0 & S_2 & 0 & 0 \\
0 & 0 & 0 & 0 & 0 & S_{-1} & 0 & 0 & S_1 & 0 & S_2 & 0 \\
0 & 0 & 0 & 0 & 0 & S_{-1} & 0 & 0 & S_1 & 0 & S_2 & 0 \\
0 & 0 & 0 & 0 & 0 & S_{-1} & 0 & 0 & S_1 & 0 & S_2 & 0
\end{pmatrix},$$

acting on function vectors of the form

$$(f_{2,1}, f_{2,-2}, f_{2,-1}, f_{1,-2}, f_{1,-1}, f_{1,2}, f_{-1,-2}, f_{-1,1}, f_{-1,2}, f_{-2,1}, f_{-2,2}, f_{-2,-1})^{\top}$$

with

$$f_{a,b}\colon S_a.I_b \to \mathbb{C}\,.$$

In (14), each entry of the form S_j indicates the operator $\tau_s(S_j)$. The matrix representation of $\mathcal{L}_s$ in (14) shows that each entry in (13) is changed for a 3×3-matrix containing mostly zeros.

Let $n \in \mathbb{N}$, $s \in \mathbb{C}$. We now thicken the intervals in $\mathcal{I}_n$ to a suitable family of domains in $\mathbb{C}$ so that we can find a good function space H on which the transfer operators $\mathcal{L}_s$ ($s \in \mathbb{C}$) act and satisfy the relation $Z_X(s) = \det(1 - \mathcal{L}_s)$.

To that end we call, for any $n \in \mathbb{N}_0$, a collection $\mathcal{E}_n := \{E_w \ : \ w \in \mathcal{W}_n\}$ of subsets of $\mathbb{C}$ a *family of admissible neighborhoods for $\mathcal{I}_n$* if for each $w \in \mathcal{W}_n$ the set E_w is an open, bounded and convex subset of $\mathbb{C}$ with $I_w \subseteq E_w$, the elements of $\mathcal{E}_n$ are pairwise disjoint, and

- in case that $n = 0$, we have
$$S_w^{-1}.\overline{E}_v \subseteq E_w$$
  whenever $w \neq -v$, and
- if $n \geq 1$, we have
$$S_{-w_1}^{-1}.\overline{E}_v \subseteq E_w$$
  whenever $w = (w_1, v_1, \ldots, v_{n-1}, -v_n)$.

For any open subset D of $\mathbb{C}$ we let $H(D)$ denote an "admissible" Banach or Hilbert space of functions $D \to \mathbb{C}$. Admissible spaces include, e.g., the Hilbert–Bergman spaces and the disk algebras from Section 2.4 as well as Hilbert–Hardy spaces. For a wider-ranging notion of admissibility see [BJ08]. In the forthcoming article in which we will discuss the validity, error estimates and convergence rates of the method of domain-refined Lagrange–Chebyshev approximation we will use Hilbert–Hardy spaces over ellipses. For any family $\mathcal{E}_n$ of admissible neighborhoods of $\mathcal{I}_n$ we set

$$H(\mathcal{E}_n) := \bigoplus_{w \in \mathcal{W}_n} H(E_w)\,.$$

Theorem 3.4. *Let $n \in \mathbb{N}_0$.*

(i) *There exists an admissible family of neighborhoods $\mathcal{E}_n$ of $\mathcal{I}_n$.*

(ii) *For every admissible family $\mathcal{E}_n$ of neighborhoods of $\mathcal{I}_n$, the transfer operator $\mathcal{L}_s$ extends to an operator $\mathcal{L}_s$ on $H(\mathcal{E}_n)$.*

(iii) *The operator $\mathcal{L}_s$ on $H(\mathcal{E}_n)$ is trace class (or nuclear of order 0) and its Fredholm determinant represents the Selberg zeta function. Thus, for all $s \in \mathbb{C}$ we have*

$$Z(s) = \det(1 - \mathcal{L}_s).$$

Proof. To establish (i) we let, for any $w \in \mathcal{W}_n$, the set E_w denote the open disk in $\mathbb{C}$ with center in $\mathbb{R}$ that satisfies $E_w \cap \mathbb{R} = I_w$. A straightforward calculation, taking advantage of the fact that Moebius transformations preserve disks, shows that $\{E_w\}_{w \in \mathcal{W}_n}$ is a family of admissible neighborhoods of $\mathcal{I}_n$. Since for $n = 0$, $\mathcal{E}_0$ being a family of disks and $H(\mathcal{E}_0)$ being chosen as Hilbert–Bergman spaces, the validity of (ii) and (iii) is known (both statements follow directly from [GLZ04]), claims (ii) and (iii) for arbitrary $n \in \mathbb{N}$, arbitrary families $\mathcal{E}_n$ of admissible neighborhoods of $\mathcal{I}_n$ and arbitrary admissible function spaces $H(\mathcal{E}_n)$ now follow either directly from [FP20] or with obvious adaptions. (Establishing the existence of a family of ellipses satisfying (i) is a non-trivial matter and will be discussed in detail in the forthcoming follow-up article.) $\square$

4. Lagrange–Chebyshev approximation

Let X be a Schottky surface,

$$\mathcal{S} = \left(q, \left(D_k \right)_{k \in I_G}, \left(S_k \right)_{k \in I_G} \right)$$

a choice of Schottky data for X, $n \in \mathbb{N}_0$ and $\mathcal{E}_n$ a family of admissible neighborhoods of $\mathcal{I}_n$ such that for each $w \in \mathcal{W}_n$, the set E_w is an ellipse with foci on the boundary points of the interval I_w, let $H(\mathcal{E}_n)$ be the Hilbert–Hardy space, and let $\mathcal{L}_s$ denote the transfer operator family associated to $\mathcal{S}$, considered as an operator on $H(\mathcal{E}_n)$. We recall that the Selberg zeta function Z_X equals the Fredholm determinant of $(\mathcal{L}_s)_{s \in \mathbb{C}}$, thus, for all $s \in \mathbb{C}$ we have $Z_X(s) = \det(1 - \mathcal{L}_s)$.

The Lagrange–Chebyshev approach for the numerical calculation of the Selberg zeta function consists of three basic steps:

(i) expand functions in $H(\mathcal{E}_n)$ in Chebyshev series, and use Gauss–Chebyshev quadrature to approximate the integrals in the coefficients,

(ii) describe the action of $1 - \mathcal{L}_s$ on the Chebyshev series, thus on the Chebyshev polynomials, and approximate these actions in the sense of Lagrange, resulting in an approximation by a finite-dimensional matrix,

(iii) approximate $Z_X(s)$ by the determinant of this matrix.

In steps (i) and (ii) the ideas of Lagrange and Chebyshev come into play, as we use a Chebyshev expansion to construct Lagrange interpolating polynomials. Steps (ii) and (iii) are reminiscent of Nyström's discretization scheme for Fredholm integral equations [Nys30], which leads to a highly efficient numerical method for the evaluation of Fredholm determinants of integral operators [Bor10].

4.1. **Interpolating polynomials.** A function f defined real-analytically in the neighborhood of the real interval $[-1, 1]$ can be expanded in terms of Chebyshev polynomials of the first kind,

$$
(15) \qquad f(x) = \mu_0 + 2 \sum_{k=1}^{\infty} \mu_k T_k(x), \qquad (x \in [-1, 1])
$$

with polynomials

$$
(16) \qquad T_k(x) := \cos(k \arccos(x))
$$

and expansion coefficients

$$
(17) \qquad \mu_k = \int_{-1}^{1} \frac{f(x) T_k(x)}{\pi \sqrt{1 - x^2}} \, dx \, .
$$

These integrals can be approximated using Gauss–Chebyshev quadrature,

$$
(18) \qquad \int_{-1}^{1} \frac{g(x)}{\pi \sqrt{1 - x^2}} \, dx \approx \sum_{j=1}^{N} w_j \, g(x_j) \, ,
$$

with points and weights

$$
(19) \qquad x_j = \cos\left(\frac{2j - 1}{2N} \pi\right), \qquad w_j = \frac{1}{N}, \qquad j = 1, \dots, N \, .
$$

For the expansion coefficients this leads to

$$
(20) \qquad \mu_k \approx \sum_{j=1}^{N} w_j \, T_k(x_j) \, f(x_j) \, .
$$

Hence, we can define a Chebyshev kernel $K_M(x, y)$ and approximate the function f by its values at the quadrature points x_j,

$$
(21) \qquad
\begin{aligned}
K_M(x, y) &= \frac{1}{M} \left[T_0(x) T_0(y) + 2 \sum_{k=1}^{M-1} T_k(x) T_k(y) \right] , \\
f(x) &\approx \frac{M}{N} \sum_{j=1}^{N} K_M(x, x_j) \, f(x_j) \, .
\end{aligned}
$$

Which order M should be used for the kernel K_M? The approximation in (21) is a polynomial of degree $M - 1$, which is uniquely defined specifying $N = M$ data points. In addition, we notice that inserting the definitions of $T_k(x)$, x_j and w_j into (20) leads to

$$
(22) \qquad \mu_k = \frac{1}{N} \sum_{j=1}^{N} \cos\left(\frac{\pi}{N} k(j - \tfrac{1}{2})\right) f(x_j) \quad \text{with} \quad k = 0, \dots, N - 1 \, ,
$$

i.e., a discrete cosine transform of type II [ANR74, Str99]. Its inverse is the discrete cosine transform of type III, which coincides with the Chebyshev expansion (21) truncated at order $M = N$ and evaluated at the points $x = x_j$,

$$
(23) \qquad f(x_j) = \mu_0 + 2 \sum_{k=1}^{N-1} \mu_k \cos\left(\frac{\pi}{N} k(j - \tfrac{1}{2})\right) \quad \text{with} \quad j = 1, \dots, N \, .
$$

Truncation at order $M = N$ is therefore a natural and consistent choice, which leads to

$$K_N(x_i, x_j) = \delta_{ij}\,,\tag{24}$$

and (21) then represents a Lagrange interpolation polynomial which is exact at the quadrature points x_j. The approximation error in (21) with $M = N$ equals

$$\frac{f^{(N)}(\xi_x)}{N!}\Phi_N(x)$$

with $\Phi_N(x) = \prod_{j=1}^{N}(x - x_j)$ and appropriate $\xi_x \in I$. Compared to other choices of the collocation points, the interpolation with Chebyshev quadrature points x_j has the advantage to minimize the maximum magnitude of $\Phi_n(x)$. See, e.g., [DB08, Riv74].

For real-analytic functions f defined in the neighborhood of a generic interval $[a, b]$ we can rescale linearly,

$$[a, b] \ni y = c + rx \quad \text{with} \quad x \in [-1, 1],\ c = \frac{a + b}{2},\ r = \frac{b - a}{2}\,.\tag{25}$$

This leads to the approximations

$$
\begin{aligned}
f(c + rx) &\approx \sum_{j=1}^{N} K_N(x, x_j)\, f(c + rx_j) \qquad \text{or} \\
f(y) &\approx \sum_{j=1}^{N} K_N[(y - c)/r, (y_j - c)/r]\, f(y_j)\,.
\end{aligned}
\tag{26}
$$

4.2. Discretization of the transfer operator.
Each matrix coefficient $\mathcal{L}_{s,v,w}$, $v, w \in \mathcal{W}_n$, of the transfer operator $\mathcal{L}_s$ is either the zero operator or an operator $\tau_s(S_k)$, $k \in I_G$, applied to functions f_w on a neighborhood (here, an ellipse) of the interval I_w resulting in functions f_v on a neighborhood of the interval I_v. See Proposition 3.2. Each such matrix coefficient of $\mathcal{L}_s$ can be discretized using (21), i.e., approximated by a finite $N \times N$-matrix. Since all collocation points are contained in the intervals, we may and shall restrict the further discussion to (real-analytic) functions on these intervals, ignoring their extension to complex neighborhoods.

Let $I_w, I_v \in \mathcal{I}_n$ be intervals and let S_k, $k \in I_G$, be one of the generators. Denote the centers and radii of the intervals by c_w, c_v and r_w, r_v, respectively. The N-point approximation $f_w^{(N)}$ of a function $f_w \in C^\omega(I_w; \mathbb{C})$ is then given by

$$
\begin{aligned}
f_w^{(N)}(y) &= \sum_{j=1}^{N} K_N[(y - c_w)/r_w, (y_j - c_w)/r_w]\, f_w(y_j), \quad \text{with} \\
y_j &= c_w + r_w x_j,\quad x_j = \cos\left(\tfrac{2j-1}{2N}\pi\right),\quad j = 1, \ldots, N\,.
\end{aligned}
\tag{27}
$$

Applying the matrix coefficient $\mathcal{L}_{s,v,w}$ to $f_w^{(N)}$ we obtain either zero or

$$
\begin{aligned}
\mathcal{L}_{s,v,w}\, f_w^{(N)}(y) &= \tau_s(S_k) f_w^{(N)}(y) = \left(S_{-k}'(y)\right)^s f_w^{(N)}(S_{-k}.y) \\
&= \left(S_{-k}'(y)\right)^s \sum_{j=1}^{N} K_N[(S_{-k}.y - c_w)/r_w, (y_j - c_w)/r_w]\, f_w(y_j),
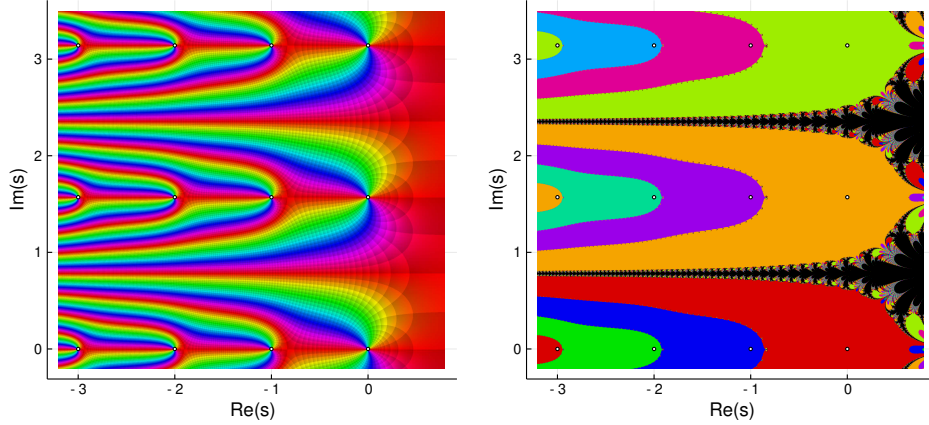\end{aligned}
\tag{28}
$$

FIGURE 4. Phase plot of $Z_X(s)$ (left) and Newton fractal (right) for the hyperbolic cylinder with funnel width 4.

which is a function f_v on I_v that we can evaluate at the quadrature points

$$(29) \qquad y_i = c_v + r_v x_i \quad \text{with} \quad x_i = \cos\left(\tfrac{2i-1}{2N}\pi\right), \quad i = 1, \dots, N.$$

The order-N discretization $\mathcal{L}_{s,v,w}^{(N)}$ of $\mathcal{L}_{s,v,w}$ is the linear operator which maps function values at quadrature points in I_w, $f_w(c_w + r_w x_j \in I_w)$, to function values at quadrature points in I_v, $f_v(c_v + r_v x_i \in I_v)$. Its $N \times N$-matrix elements are given by

$$(30)$$
$$\left(\mathcal{L}_{s,v,w}^{(N)}\right)_{i,j} = \begin{cases} \left(S_{-k}'(c_v + r_v x_i)\right)^s K_N\left[\dfrac{S_{-k}.(c_v + r_v x_i) - c_w}{r_w}, x_j\right] & \text{if } S_{-k}.I_v \subseteq I_w \\ 0 & \text{otherwise.} \end{cases}$$

To get an order-N discretization $\mathcal{L}_s^{(N)}$ of the full transfer operator we replace each matrix coefficient $\mathcal{L}_{s,v,w}$ by its discretization $\mathcal{L}_{s,v,w}^{(N)}$. This results in a big square matrix constructed from many $N \times N$-blocks, most of which are zero. The full dimension of the vector space the discretization $\mathcal{L}_s^{(N)}$ is acting on is $2q(2q-1)^n N$.

4.3. Numerical evaluation of matrix determinants.

The transfer operator consists of an s-dependent part and a static part, which only depends on the given intervals and group generators. When $\mathcal{L}_s^{(N)}$ is evaluated numerically for different values of s, only the first part needs to be changed, the second can be re-used.

To calculate the numerical value of the Selberg zeta function Z_X at s, thus $Z_X(s) = \det(1 - \mathcal{L}_s)$, we construct the matrix $1 - \mathcal{L}_s^{(N)}$ and calculate its determinant with some standard numerical library routine. Such routines are usually based on LU-factorization of the matrix, and available code is highly optimized and fast. For dense matrices (low domain refinement) we can use `zgetrf` from LAPACK, for sparse matrices (high domain refinement) SuiteSparse offers the `umfpack` family of functions. Higher level languages such as Python, Sage or Julia offer simple wrapper functions for matrix determinants (and for $\log\det[.]$), which select and call one of the above optimized libraries.

4.4. **Finding zeros of Z_X.** With a stable algorithm for $Z_X(s)$ at hand we are now in the position to calculate resonances, which are zeros of Z_X. A simple and efficient algorithm for this task is Newton's method, which is based on the iteration

$$(31) \qquad s \to s - \frac{Z_X(s)}{Z'_X(s)} \,.$$

The absolute value of $Z_X(s)$ grows exponentially with $-\operatorname{Re} s$, i.e., there is always strong gradient from negative $\operatorname{Re} s$ to positive. We observe that for every zero s_0 with $\operatorname{Re} s_0 > c$ there is a curve of constant phase, $\operatorname{Im} \log(Z_X(s)) = \phi$, which starts at $s = s_0$ and crosses the line $s = c + i\mathbb{R}$ eventually. This behavior is reflected in the Newton fractal of $Z_X(s)$: For every root s_0 with $\operatorname{Re} s_0 > c$ the basin of attraction of the Newton map intersects the line $c + i\mathbb{R}$ at least once. In Figure 4 we illustrate this behavior for the simplest Schottky surface, i.e., for the hyperbolic cylinder.

To locate all zeros s_0 with $\operatorname{Re} s_0 > c$ we therefore choose a sufficiently dense set of starting values along the line $c + i\mathbb{R}$ and iterate Newton's method until it converges or fails. The set of zeros we find can contain duplicates, which we need to filter out, and we may miss zeros if the set of starting values is not dense enough.

Unless the convergence rate is analyzed in detail, Newton's method cannot determine the order of a zero. We could use the argument principle in a small neighborhood of a zero to find the order. However, except for highly symmetric surfaces most of the resonances appear to be simple zeros. For topological zeros on the real line the order is known.

5. Examples

We now illustrate the performance of the domain-refined Lagrange–Chebyshev approximation with plots of the resonance spectra of various Schottky surfaces.

5.1. **Three-funnel surfaces.** We start with three-funnel surfaces which were studied already in Borthwick's seminal paper [Bor14] and later discussed in his book [Bor16]. These can be generated using matrices of the form

$$(32) \qquad S(l,a) = \begin{pmatrix} \cosh(l/2) & a\sinh(l/2) \\ a^{-1}\sinh(l/2) & \cosh(l/2) \end{pmatrix} \quad \text{with} \quad S(l,a)^{-1} = S(l,-a) \,.$$

If we define the boundary of a disk D by the condition $S(l,a)'(z) = 1$, its center is at $-a\coth(l/2)$ and the radius equals $|a/\sinh(l/2)|$. The transformation $z \to S(l,a).z$ maps the exterior of D to the inside of a disk $\tilde{D}$ of the same radius but centered at $+a\coth(l/2)$. The geodesic between the boundaries of the two disks has length l.

Using two generators of this type,

$$(33) \qquad S_1 = S(\ell_1, 1) \quad \text{and} \quad S_2 = S(\ell_2, a_2) \,,$$

we glue the corresponding pairs of disks, D_1, D_{-1} and D_2, D_{-2}, to obtain a surface with three funnels. See Figure 1. The first two funnels have widths ℓ_1 and ℓ_2, the widths of the third, ℓ_3, depends on the parameter a_2 through the condition

$$(34) \qquad \operatorname{tr}(S_1 S_{-2}) = -2\cosh(\ell_3/2) \,,$$

which ensures that the geodesics between D_1 and D_2 and between D_{-1} and D_{-2} each have length $\ell_3/2$. Solving (34) for a_2 we define a function $A(\ell_1, \ell_2, \ell_3)$ for later
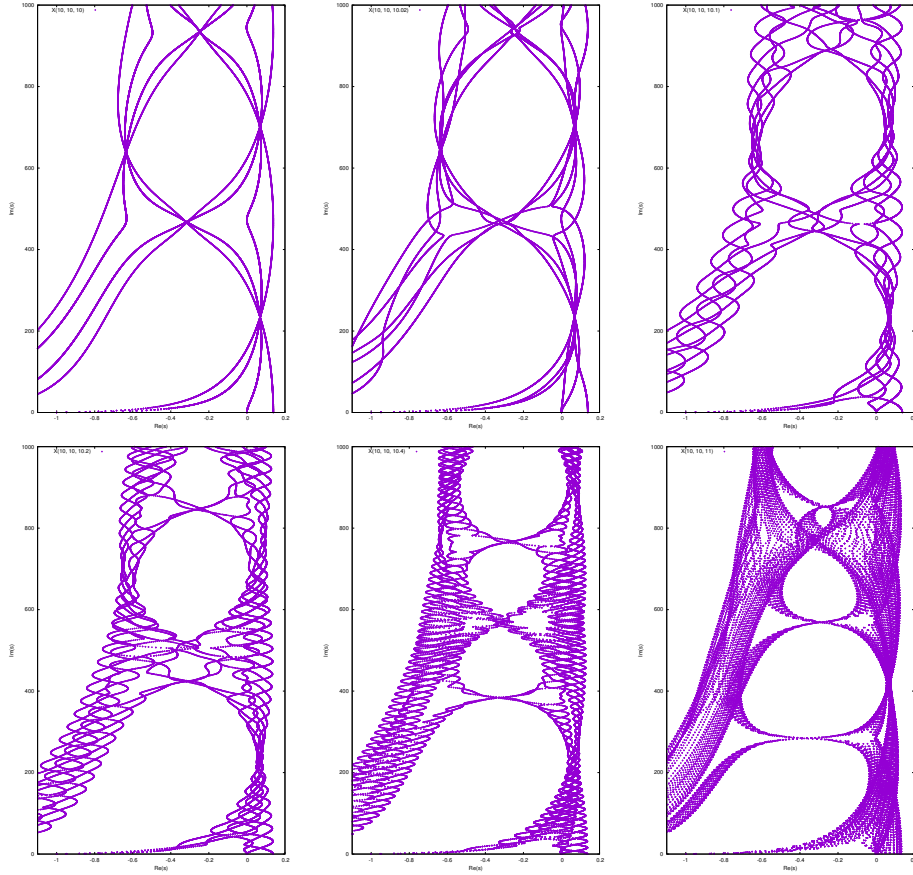
FIGURE 5. Evolution of the resonance spectrum for the three-funnel surface $X(10, 10, \ell)$ for $\ell = 10, 10.02, 10.1, 10.2, 10.4$ and 11.

use and obtain

(35)
$$a_2 = A(\ell_1, \ell_2, \ell_3) := d - \sqrt{d^2 - 1} \quad \text{with}$$
$$d = \frac{\cosh(\ell_1/2)\cosh(\ell_2/2) + \cosh(\ell_3/2)}{\sinh(\ell_1/2)\sinh(\ell_2/2)}.$$

Following Borthwick, we denote such a surface by $X(\ell_1, \ell_2, \ell_3)$. The disks $D_{\pm 1}$ and $D_{\pm 2}$ form the starting point for domain-refinement, as illustrated in Figure 3.

As a first test, in Figure 5 we reconsider the series of resonance spectra for $X(10, 10, \ell)$ first studied by Borthwick [Bor14]. However, we extend the range of the spectral parameter from $\operatorname{Re} s \geq 0$ to $\operatorname{Re} s > -1.1$. This reveals many new and fascinating structures. For instance, the chains of resonances seem to oscillate between strands formed by multiple chains. Also, it looks as if the chains start at the topological zeros $s = -\mathbb{N}$ and the Hausdorff dimension δ of the limit set $\Lambda(X)$ of X. These features become even more apparent in Figure 6 where we study the spectrum of $X(6, 6, 6)$ and extend the range of the spectral parameter even further to $\operatorname{Re} s > -2.1$.
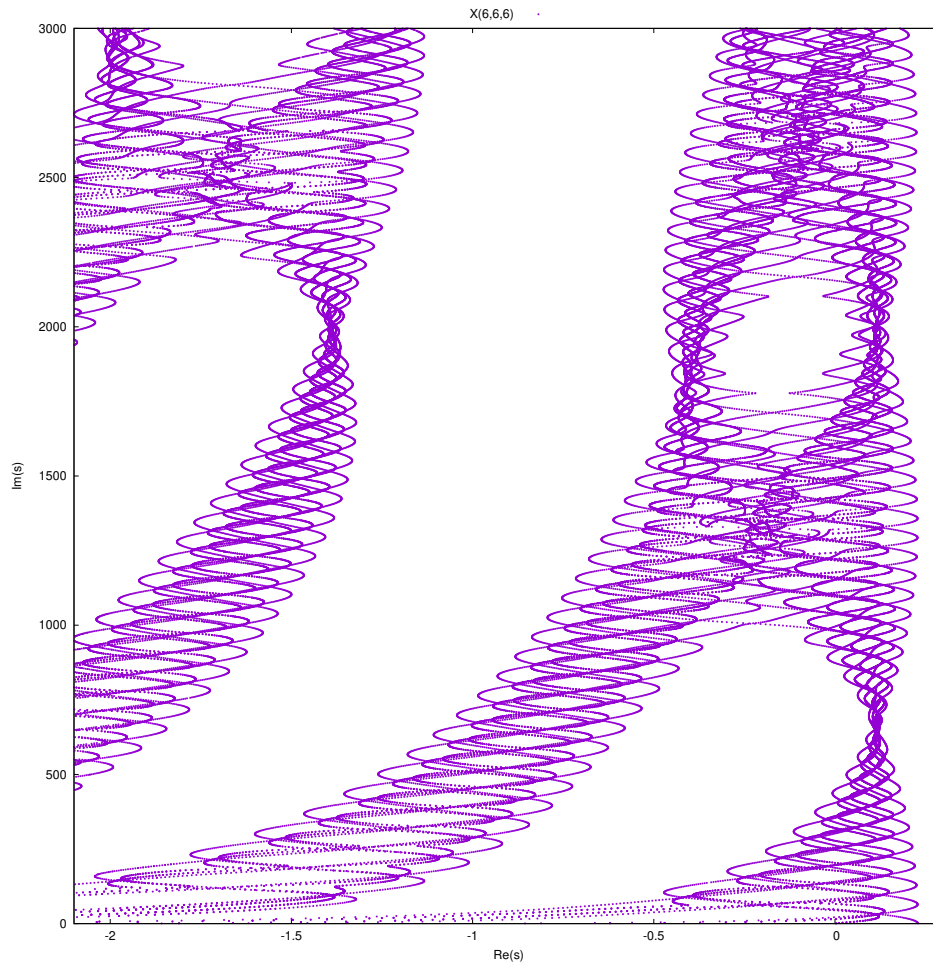
FIGURE 6. Resonance spectrum for the three-funnel surface $X(6, 6, 6)$.

An aspect which did not receive much attention in previous studies is the multiplicity of the resonances. We observe that for symmetric three-funnel surfaces some of the zeros of $Z_X(s)$ have multiplicity 2. In Figure 7 we zoom in on the spectrum of the surface $X(7, 7, 7)$ and show a phase plot of the function $Z_X(s)$ with its argument coded in color. In each group of four zeros there are two where the color wheel is circled twice. This corresponds to multiplicity two. Interestingly, the Venkov–Zograf factorization used by Borthwick–Weich does not split up these two-fold zeros, compare [BW16, Figure 9]. If the symmetry if broken, the two-fold zeros split up and all resonances have multiplicity one, see Figure 5.

5.2. **n-funnel surfaces.** For surfaces with more than three funnels of widths $\ell_1, \ldots, \ell_n$, we extend the above construction by adding further generators $S(l_k, a_k)$ of the type (32) and corresponding pairs of disks $D_{\pm k}$. In total we need $n-1$ generators (and their inverses) for n funnels. The l-parameters of the first and last generator
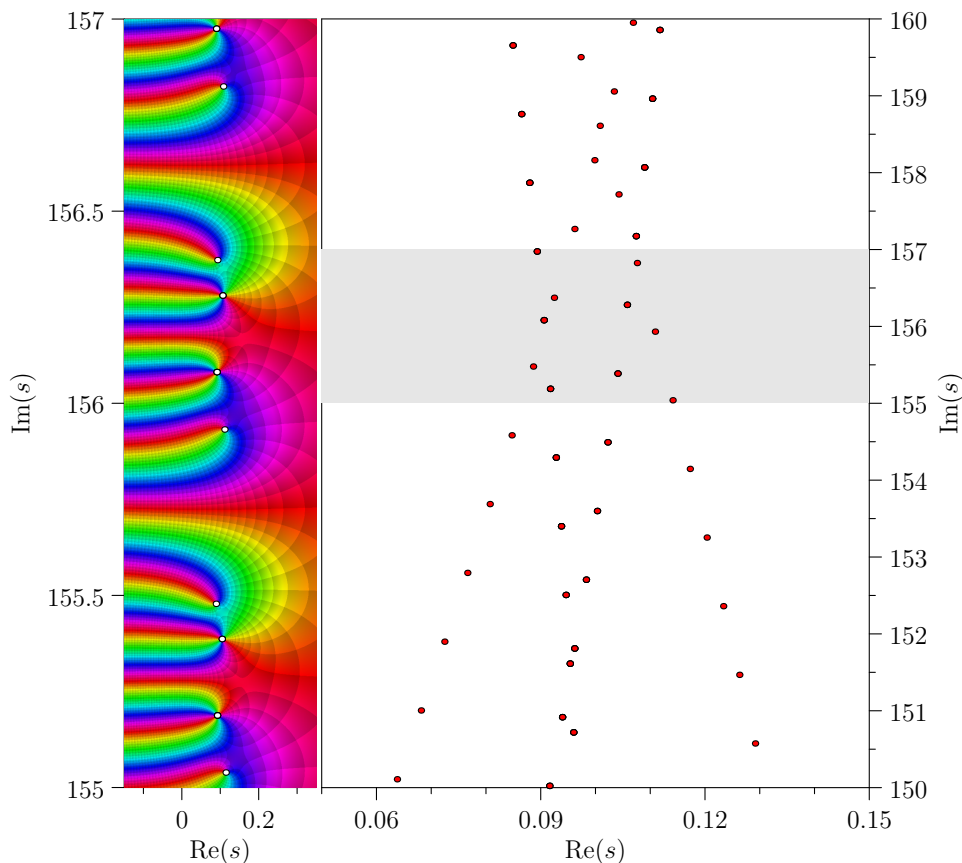
FIGURE 7. Right: Zoom in on the resonance spectrum of the three-funnel surface $X(7,7,7)$. Left: Phase plot of $Z_X(s)$ with all zeros from the shaded area, indicating that some have multiplicity two.

determine the funnel-width of the first and last funnel, $l_1 = \ell_1$ and $l_{n-1} = \ell_n$, the l's of the other generators are free parameters describing a waist circumference. The widths of the intermediate funnels can be fixed using the function A defined in (35) above. For given l_k we build up the parameters a_k multiplicatively,

$$(36) \qquad\qquad a_1 = 1, \quad a_{k+1} = A(l_k, l_{k+1}, \ell_{k+1})\, a_k\,.$$

To make the surface symmetric, we need to tune the "inner" l-parameters such that equivalent waist circumferences are equal. This can be done numerically.

Figure 8 shows this construction for a symmetric four-funnel surface. Here the width of all four funnels is 3 and symmetry requires $l_2 = 4.853373$ for the inner generator S_2. Only then the lengths of the geodesics $D_1 \leftrightarrow D_3$ and $D_{-1} \leftrightarrow D_{-3}$ add up to l_2 and the two waists have equal circumference (red dashed lines). For surfaces with more funnels the construction is similar, but there are more waistlines to match.
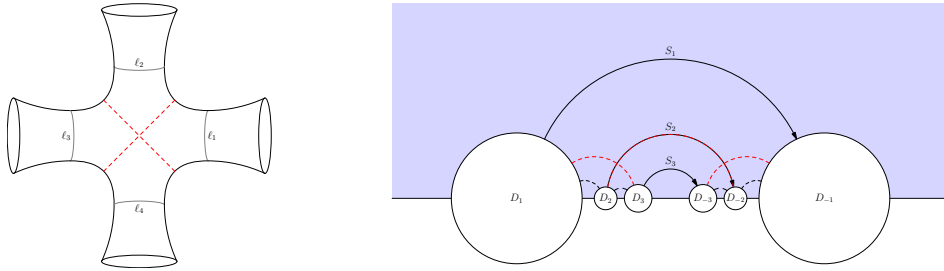
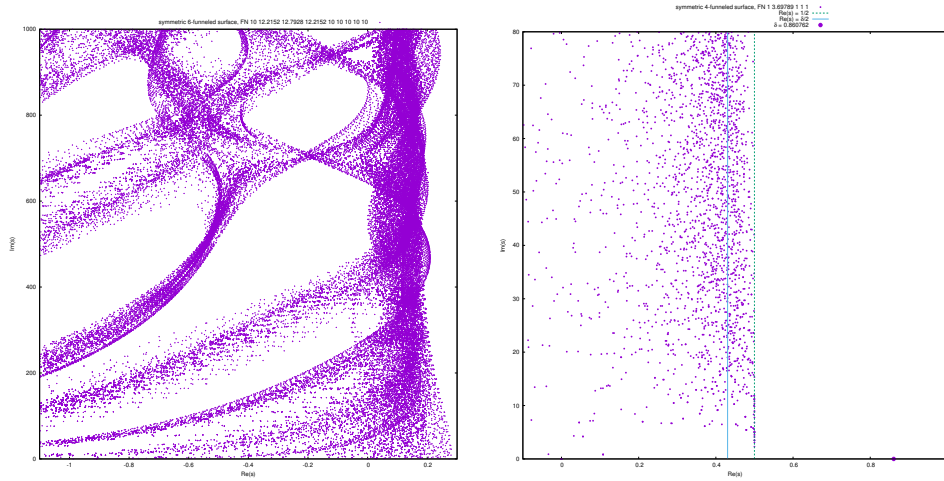FIGURE 8. Construction of a symmetric four-funnel surface.

FIGURE 9. Spectra of symmetric n-funnel surfaces. Left: Surface
with 6 funnels all of width 10. Right: Surface with 4 funnels all of
width 1.

Our construction has the advantage, that the size difference between disks is
not too pronounced and that the whole arrangement is more symmetric. This makes
it better suited for the Langrange–Chebyshev approach.

In Figure 9 we show resonance spectra for symmetric n-funnel surfaces. The
data on the left is for a surface with 6 funnels all of width 10. Its construction
requires 5 generators and their inverses, corresponding to 5 pairs of disks. The data
on the right is for a surface with 4 funnels, but their width is only 1. For such
narrow funnels the Hausdorff dimension of the limit set is approaching a value close
to one, $\delta = 0.86076$ in this case. The data clearly shows that there are no resonances
with $\operatorname{Im} s \neq 0$ and $\operatorname{Re} s > 1/2$. Instead, some resonances accumulate close to the
line $\operatorname{Re} s = 1/2$, indicated by the green dashed line. The data also seems to support
conjectures that the density of resonances has a maximum near $\operatorname{Re} s = \delta/2$ indicated
by the blue solid line in the figure [JN12].

We note that small funnel widths or large δ are situations where domain-
refinement becomes important. The surface with 6 funnels of width 10 was simulated
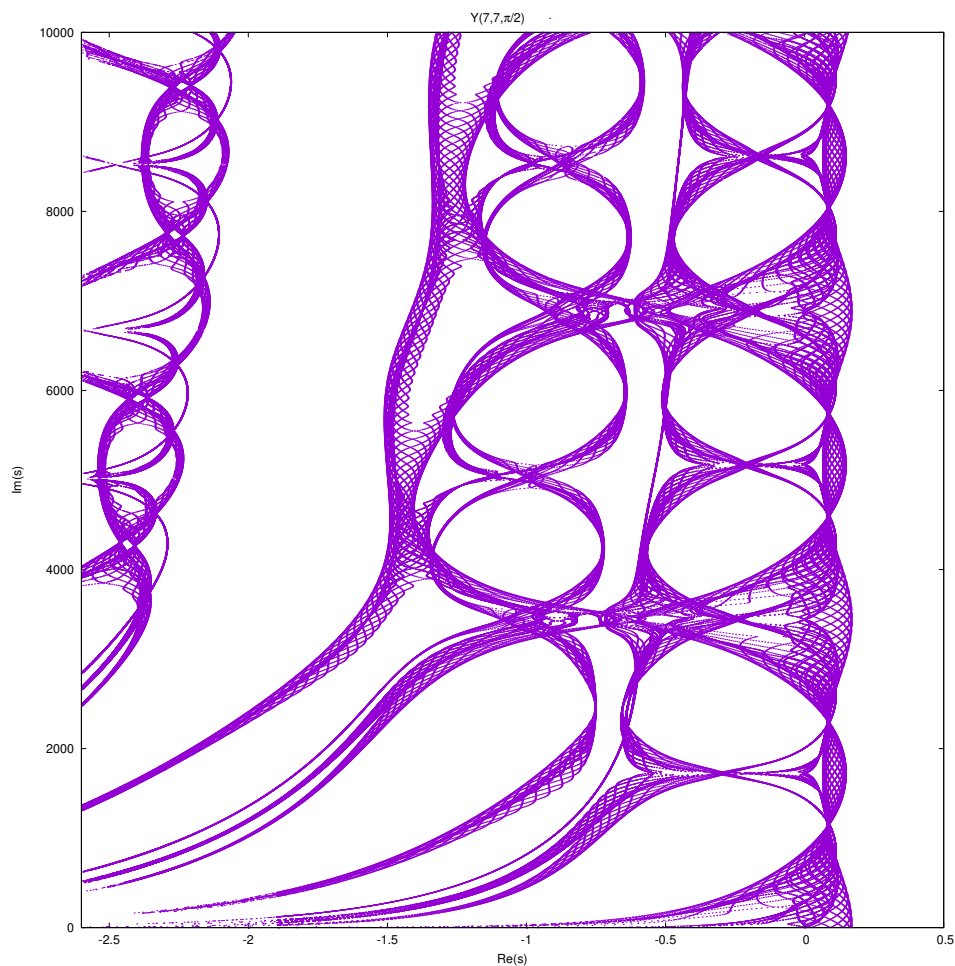with a subdivision level of $n = 1$ only, and could presumably be solved without

FIGURE 10. Resonance spectrum for the funneled torus $Y(7, 7, \pi/2)$.

domain refinement. The 4-funnel surface with narrow funnels, on the other hand, required a subdivision level of $n = 3$. We will discuss such convergence properties in more detail in a forthcoming article.

5.3. **Funneled tori.** As examples of surfaces of genus 1, we reconsider tori with one attached funnel. These were also first studied by Borthwick [Bor14] and constructed from the two generators

$$
(37) \quad
\begin{aligned}
\tilde{S}_1 &= \begin{pmatrix} e^{\ell_1/2} & 0 \\ 0 & e^{-\ell_1/2} \end{pmatrix}, \\
\tilde{S}_2 &= \begin{pmatrix} \cosh(\ell_2/2) - \cos(\phi)\sinh(\ell_2/2) & \sin^2(\phi)\sinh(\ell_2/2) \\ \sinh(\ell_2/2) & \cosh(\ell_2/2) + \cos(\phi)\sinh(\ell_2/2) \end{pmatrix}.
\end{aligned}
$$

For our algorithm this choice is not usable, since one of the corresponding disks includes the point at infinity. We can avoid this problem by rotating the above generators by $\pi/8$, i.e., we use
(38)
$$S_1 = R(\tfrac{\pi}{8})\, \tilde{S}_1\, R(-\tfrac{\pi}{8})\,, \quad S_2 = R(\tfrac{\pi}{8})\, \tilde{S}_2\, R(-\tfrac{\pi}{8})\,, \quad R(\psi) = \begin{pmatrix} \cos(\psi) & -\sin(\psi) \\ \sin(\psi) & \cos(\psi) \end{pmatrix}.$$

Our convention $S'(z) = 1$ then results in disks $D_{\pm 1}$, $D_{\pm 2}$, which for $\phi = \pi/2$ have equal size, and small size differences otherwise. In case that the ℓ's are too small, this construction can lead to invalid, overlapping disks, and some other choice is required. Following Borthwick, we denote such surfaces by $Y(\ell_1, \ell_2, \phi)$. In Figure 2 we illustrate the construction of $Y(4, 4, \pi/2)$.

The resonance spectrum of funneled tori is more delicate with many fine details, in particular, when the surface is symmetric. In Figure 10 we show the spectrum of $Y(7, 7, \pi/2)$. Compared to previous studies, we were able to increase the range of the spectral parameter to $\operatorname{Re} s > -2.6$.

6. Algorithms

In this section we list the algorithms for the calculation of resonances.

Algorithm 1 Construct $N \times N$ sub-block $\mathcal{L}_s^{(N)}$ of full transfer operator.

1: **function** LBLOCK(N, I_v, I_w, g)
2:     $c_v, r_v \leftarrow$ center & radius of I_v
3:     $c_w, r_w \leftarrow$ center & radius of I_w
4:     **for** $i = 1, \ldots, N$ **do**
5:         $x_i \leftarrow \cos\left(\tfrac{\pi}{N}(i - \tfrac{1}{2})\right)$
6:     **end for**
7:     **for** $i = 1, \ldots, N$ **do**
8:         **for** $j = 1, \ldots, N$ **do**
9:             $m_{ij} \leftarrow K_N[(g(c_v + r_v x_i) - c_w)/r_w, x_j]$
            $f_i \leftarrow g'(c_v + r_v x_i)$
10:         **end for**
11:     **end for**
12:     **return** $[f, m]$ $\triangleright$ $f : N$-vector, $m : N \times N$-matrix
13: **end function**

Algorithm 2 Construct index set $\mathcal{W}_n$.

1: **function** INDEXSET(q, n)
2:     $\mathcal{W}_n \leftarrow [\,]$
3:     $I_G \leftarrow [-q, \ldots, -1, 1, \ldots, q]$
4:     $r \leftarrow \begin{cases} 1 & n < 2 \\ -1 & \text{otherwise} \end{cases}$
5:     **if** $n = 0$ **then**
6:         **for** $k \in I_G$ **do**
7:             $\mathcal{W}_n \leftarrow$ APPEND$(\mathcal{W}_n, [k])$
8:         **end for**
9:     **else**
10:         **for** $w \in \mathcal{W}_{n-1} =$ INDEXSET$(q, n-1)$ **do**
11:             **for** $k \in I_G$ **do**
12:                 **if** $r \cdot k \neq$ FIRST(w) **then**
13:                     $\tilde{w} \leftarrow$ PREPEND(w, k)
14:                     $\mathcal{W}_n \leftarrow$ APPEND$(\mathcal{W}_n, \tilde{w})$
15:                 **end if**
16:             **end for**
17:         **end for**
18:     **end if**
19:     **return** $\mathcal{W}_n$ ▷ $2q(2q-1)^n$-element array of $(n+1)$-element index sets.
20: **end function**

Algorithm 3 Build domain-refined transfer operator $\mathcal{L}_s^{(N)}$.

1: **function** LPARTS$(N, q, n, [D_{-q}, \ldots, D_{-1}, D_1, \ldots, D_q])$
2:     $I_G \leftarrow \{-q, \ldots, -1, 1, \ldots, q\}$
3:     $S_k \leftarrow$ generator mapping outside of D_k to inside of $D_{-k} \, \forall k \in I_G$
4:     $I_k \leftarrow D_k \cap \mathbb{R} \, \forall k \in I_G$
5:     $\mathcal{W}_n \leftarrow$ INDEXSET(q, n)
6:     **for** $v = (v_1, \ldots, v_n, \ell_v) \in \mathcal{W}_n$ **do**
7:         **for** $w = (w_1, \ldots, w_n, \ell_w) \in \mathcal{W}_n$ **do**
8:             **if** $w = (w_1, v_1, \ldots, v_{n-1}, -v_n)$ **then**
9:                 $I_v \leftarrow S_{v_1} \cdots S_{v_n}.I_{\ell_v}$
10:                $I_w \leftarrow S_{w_1} \cdots S_{w_n}.I_{\ell_w}$
11:                $[F_{vw}, M_{vw}] \leftarrow$ LBLOCK(n, I_v, I_w, S_{-w_1})
12:             **else**
13:                $[F_{vw}, M_{vw}] \leftarrow [1, 0]$
14:             **end if**
15:         **end for**
16:     **end for**
17:     **return** $[F, M]$ ▷ $\begin{array}{l} F : d \times d \text{ array of } N\text{-vectors} \\ M : d \times d \text{ array of } N \times N\text{-matrices} \\ d = \dim(\mathcal{W}_n) = 2q(2q-1)^n \end{array}$
18: **end function**

Algorithm 4 Evaluate $Z(s) = \det(1 - \mathcal{L}_s^{(N)})$ using pre-calculated parts.

1: **function** Z$(s, N, q, n, [F, M])$
2: $\quad \mathcal{W}_n \leftarrow$ INDEXSET(q, n)
3: $\quad d \leftarrow \dim(\mathcal{W}_n)$
4: $\quad$ **for** $v \in \mathcal{W}_n$ **do**
5: $\quad\quad$ **for** $w \in \mathcal{W}_n$ **do**
6: $\quad\quad\quad L_{vw} \leftarrow M_{vw} \operatorname{diag}(F_{vw}^s)$ $\quad \triangleright$ F_{ij} is N-vector; exponentiate elements L_{vw}, M_{vw} are $N \times N$ matrices
7: $\quad\quad$ **end for**
8: $\quad$ **end for**
9: $\quad$ **return** $\det\left(1 - \begin{bmatrix} L_{11} & \cdots & L_{1d} \\ \vdots & & \vdots \\ L_{d1} & \cdots & L_{dd} \end{bmatrix}\right)$ $\quad \triangleright$ call library for det() (LU factorization)
10: **end function**

REFERENCES

[ANR74] N. Ahmed, T. Natarajan, and K. R. Rao. *Discrete cosine transform*. IEEE Trans. Comput. (1974). **C-23**, 90–93. DOI:10.1109/t-c.1974.223784.

[APW18] A. Adam, A. Pohl, and A. Weiße. *Zero is a resonance of every Schottky surface* (2018). arXiv:1808.09239.

[BD18] J. Bourgain and S. Dyatlov. *Spectral gaps without the pressure condition*. Ann. of Math. (2) (2018). **187**, no. 3, 825–867. DOI:10.4007/annals.2018.187.3.5.

[BFM13] R. Bruggeman, M. Fraczek, and D. Mayer. *Perturbation of zeros of the Selberg zeta function for* $\Gamma_0(4)$. Exp. Math. (2013). **22**, no. 3, 217–242. DOI:10.1080/10586458.2013.776381.

[BGS11] J. Bourgain, A. Gamburd, and P. Sarnak. *Generalization of Selberg's $\frac{3}{16}$ theorem and affine sieve*. Acta Math. (2011). **207**, no. 2, 255–290. DOI:10.1007/s11511-012-0070-x.

[BJ08] O. F. Bandtlow and O. Jenkinson. *On the Ruelle eigenvalue sequence*. Ergodic Theory Dynam. Systems (2008). **28**, no. 6, 1701–1711. DOI:10.1017/S0143385708000059.

[BJP05] D. Borthwick, C. Judge, and P. A. Perry. *Selberg's zeta function and the spectral geometry of geometrically finite hyperbolic surfaces*. Comment. Math. Helv. (2005). **80**, no. 3, 483–515. DOI:10.4171/CMH/23.

[Bor10] F. Bornemann. *On the numerical evaluation of Fredholm determinants*. Math. Comp. (2010). **79**, no. 270, 871–915. DOI:10.1090/S0025-5718-09-02280-7.

[Bor14] D. Borthwick. *Distribution of resonances for hyperbolic surfaces*. Exp. Math. (2014). **23**, no. 1, 25–45. DOI:10.1080/10586458.2013.857282.

[Bor16] ———. *Spectral theory of infinite-area hyperbolic surfaces*, vol. 318 of *Progress in Mathematics*. Birkhäuser/Springer, [Cham], second edn. (2016). DOI:10.1007/978-3-319-33877-4.

[BS20] O. Bandtlow and J. Slipantschuk. *Lagrange approximation of transfer operators associated with holomorphic data* (2020). arXiv:2004.03534.

[But98]   J. Button. *All Fuchsian Schottky groups are classical Schottky groups*. In *The Epstein birthday schrift*, vol. 1 of *Geom. Topol. Monogr.* Geom. Topol. Publ., Coventry (1998). 117–125. DOI:10.2140/gtm.1998.1.117.

[BW16]   D. Borthwick and T. Weich. *Symmetry reduction of holomorphic iterated function schemes and factorization of Selberg zeta functions*. J. Spectr. Theory (2016). **6**, no. 2, 267–329. DOI:10.4171/JST/125.

[DB08]   G. Dahlquist and Å. Björck. *Numerical methods in scientific computing. Vol. I.* Society for Industrial and Applied Mathematics (SIAM), Philadelphia, PA (2008). DOI:10.1137/1.9780898717785.

[DGK14]   M. Dugave, F. Göhmann, and K. K. Kozlowski. *Low-temperature large-distance asymptotics of the transversal two-point functions of the XXZ chain*. J. Stat. Mech. Theory Exp. (2014). , no. 4, P04012, 37. DOI:10.1088/1742-5468/2014/04/p04012.

[FP20]   K. Fedosova and A. Pohl. *Meromorphic continuation of Selberg zeta functions with twists having non-expanding cusp monodromy*. Selecta Math. (N.S.) (2020). **26**, no. 1, Paper No. 9. DOI:10.1007/s00029-019-0534-3.

[Fra12]   M. Fraczek. *Character deformation of the Selberg zeta function for congruence subgroups via the transfer operator*. PhD thesis, Clausthal University of Technology (2012), 226 pp.

[Fra17]   ———. *Selberg zeta functions and transfer operators*, vol. 2139 of *Lecture Notes in Mathematics*. Springer (2017). DOI:10.1007/978-3-319-51296-9.

[GGK00]   I. Gohberg, S. Goldberg, and N. Krupnik. *Traces and determinants of linear operators*, vol. 116. Basel: Birkhäuser (2000).

[GLZ04]   L. Guillopé, K. K. Lin, and M. Zworski. *The Selberg zeta function for convex co-compact Schottky groups*. Comm. Math. Phys. (2004). **245**, no. 1, 149–176. DOI:10.1007/s00220-003-1007-1.

[GW12]   M. J. Gander and G. Wanner. *From Euler, Ritz, and Galerkin to modern computing*. SIAM Rev. (2012). **54**, no. 4, 627–666. DOI:10.1137/100804036.

[GZ95]   L. Guillopé and M. Zworski. *Upper bounds on the number of resonances for non-compact Riemann surfaces*. J. Funct. Anal. (1995). **129**, no. 2, 364–389. DOI:10.1006/jfan.1995.1055.

[GZ97]   ———. *Scattering asymptotics for Riemann surfaces*. Ann. of Math. (2) (1997). **145**, no. 3, 597–660. DOI:10.2307/2951846.

[JN12]   D. Jakobson and F. Naud. *On the critical line of convex co-compact hyperbolic surfaces*. Geom. Funct. Anal. (2012). **22**, no. 2, 352–368. DOI:10.1007/s00039-012-0154-y.

[May90]   D. H. Mayer. *On the thermodynamic formalism for the Gauss map*. Comm. Math. Phys. (1990). **130**, no. 2, 311–333. URL:http://projecteuclid.org/euclid.cmp/1104200514.

[May91]   ———. *The thermodynamic formalism approach to Selberg's zeta function for* PSL(2, **Z**). Bull. Amer. Math. Soc. (N.S.) (1991). **25**, no. 1, 55–60. DOI:10.1090/S0273-0979-1991-16023-4.

[MM87]   R. R. Mazzeo and R. B. Melrose. *Meromorphic extension of the resolvent on complete spaces with asymptotically constant negative curvature*. J. Funct. Anal. (1987). **75**, no. 2, 260–310. DOI:10.1016/0022-1236(87)90097-8.

[Nie16]   A. Nielsen. *Computation Schemes for Transfer Operators*. PhD thesis, FU Berlin (2016), 106 pp. DOI:10.17169/refubium-9756.

[NM19]   F. Naud and M. Magee. *Explicit spectral gaps for random covers of Riemann surfaces* (2019). arXiv:1906.00658.

[Nys30]   E. J. Nyström. *Über die praktische Auflösung von Integralgleichungen mit Anwendungen auf Randwertaufgaben*. Acta Math. (1930). **54**, no. 1, 185–204. DOI:10.1007/BF02547521.

[OW16]   H. Oh and D. Winter. *Uniform exponential mixing and resonance free regions for convex cocompact congruence subgroups of* SL$_2$(ℤ). J. Amer. Math. Soc. (2016). **29**, no. 4, 1069–1115. DOI:10.1090/jams/849.

[PP01]   S. J. Patterson and P. A. Perry. *The divisor of Selberg's zeta function for Kleinian groups*. Duke Math. J. (2001). **106**, no. 2, 321–390. DOI:10.1215/S0012-7094-01-10624-8. Appendix A by Charles Epstein.

[PS18]   A. Pohl and L. Soares. *Density of resonances for covers of Schottky surfaces* (2018). arXiv:1807.00299.

26

[PV19]   M. Pollicott and P. Vytnova. *Zeros of the Selberg zeta function for symmetric infinite area hyperbolic surfaces*. Geom. Dedicata (2019). **201**, 155–186. DOI:10.1007/s10711-018-0386-6.

[Riv74]   T. J. Rivlin. *The Chebyshev polynomials*. Wiley-Interscience [John Wiley & Sons], New York-London-Sydney (1974). Pure and Applied Mathematics.

[Rue78]   D. Ruelle. *Thermodynamic formalism*, vol. 5 of *Encyclopedia of Mathematics and its Applications*. Addison-Wesley Publishing Co., Reading, Mass. (1978). The mathematical structures of classical equilibrium statistical mechanics, With a foreword by Giovanni Gallavotti and Gian-Carlo Rota.

[Str99]   G. Strang. *The discrete cosine transform*. SIAM Rev. (1999). **41**, no. 1, 135–147. DOI:10.1137/S0036144598336745.

[Wor19]   C. Wormell. *Spectral Galerkin methods for transfer operators in uniformly expanding dynamics*. Numer. Math. (2019). **142**, no. 2, 421–463. DOI:10.1007/s00211-019-01031-z.

Oscar F. Bandtlow, School of Mathematical Sciences, Queen Mary University of London, London E3 4NS, UK.

Email address: `o.bandtlow@qmul.ac.uk`

Anke Pohl, University of Bremen, Department 3 – Mathematics, Bibliothekstr. 5, 28359 Bremen, Germany

Email address: `apohl@uni-bremen.de`

Torben Schick, Hauburgsteinweg 47, 61476 Kronberg, Germany

Email address: `torben.schick@adesso.de`

Alexander Weisse, Max Planck Institute for Mathematics, Vivatsgasse 7, 53111 Bonn, Germany

Email address: `weisse@mpim-bonn.mpg.de`